Experimental Mechanics (2009) 49:587–593
DOI 10.1007/s11340-008-9129-1

The Effect of Strain Rate, Specimen Geometry and Lubrication on Responses of Aluminium AA2024 in Uniaxial Compression Experiments

P. Li · C.R. Siviour · N. Petrinic

Received: 18 December 2007 / Accepted: 12 February 2008 / Published online: 1 April 2008

Abstract The ability to observe and quantify intrinsic material response to loading at different rates of strain has been improved by reducing the errors of mechanical characterisation in uniaxial compression experiments. In order to perform comparisons of the results from uniaxial compression tests used to characterise mechanical properties of aluminium alloys at different strain rates, it is necessary to reduce errors resulting from factors such as specimen design. In this study, the effects of strain rate, specimen geometry and lubrication on the compressive properties of aluminium AA2024 alloy were quantitatively investigated by measuring the mechanical behaviour of this alloy as functions of strain rate, specimen aspect ratio and lubrication condition. Both the deformation history and the failure mode were identified using low and ultrahigh speed photography. The interaction of factors influencing the measured stress-strain response was quantified, and suitable specimen aspect ratios for compression tests at different strain rates were identified.

Keywords Aluminium alloy · Compressive property · Strain rate · Dynamic loading · Surface profiling

Introduction

Heat treatable wrought aluminium alloys (e.g. AA2024) are widely used in aerospace applications due to their high strength-to-weight ratio. The complex in-service loading requires predictive modelling tools to be developed to simulate the damage resistance of components. However, a reliable modelling method is directly dependent on an accurate characterisation of the mechanical response of the material at a wide range of loading rates.

Aluminium alloys tend to have a small sensitivity to strain rate at room temperature, e.g. 3–9% increase in flow stress from quasi-static to high loading rates for AA6061-T651 alloy [1], although the effect of strain rate on stress-strain response becomes more pronounced at elevated temperatures [2, 3]. The microscopic mechanism leading to strain rate sensitivity of aluminium alloys is still a matter of debate, however dislocation movement has been linked to explain strengthening and rate dependency of the material. During deformation, dislocation movement is impeded by the finely dispersed precipitate particles in aluminium alloys. To quantify the effect of strain rate on stress-strain response [4], particularly at ambient temperatures, it is therefore necessary to minimise errors during characterisation experiments, which may occur due to factors such as specimen design and friction.

Uniaxial compression tests are commonly used to characterise the mechanical (compressive) properties of materials at strain rates ranging from 10^{-4} to 10^{4} s^{-1} [5, 6]. However, a multiaxial stress state inevitably arises in the compression test specimen owing to the presence of friction, regardless of the applied lubricant [1, 7–11]. The measured stress value is not just a function of the lubricant type but also of the specimen geometry [8, 12]. The interfacial frictional effect in a compression test can be established by [13]:

$$\overline{P} = \left(1 + \frac{\mu}{n} \cdot \frac{d}{l}\right)\sigma_y \tag{1}$$

P. Li (✉) · C.R. Siviour (SEM Member) · N. Petrinic
Impact Engineering Team,
Solid Mechanics and Materials Engineering Group,
Department of Engineering Science, University of Oxford,
Oxford OX1 3PJ, UK
e-mail: peifeng.li@eng.ox.ac.uk

where $\overline{P}$ is the applied mean pressure, μ is the coefficient of friction, n is a number (which equals 3 according to Hall et al. [1]), d and l are the diameter and length of the cylindrical specimen, respectively, and σ_y is the intrinsic yield stress of the material (when $\mu=0$). A large aspect ratio (l/d) specimen can reduce the friction and the subsequent barrelling effect in compression tests; however, this may produce shearing or even buckling deformation. Suitable specimen geometries should therefore be selected to improve the measurement accuracy. However, there is no study in the literature focusing on specimen geometry and lubrication effects on the compressive properties of aluminium alloys. In addition, there is a limited data set on the high rate properties of these alloys in general.

In this study, the post-yield compressive behaviour of AA2024 alloy was measured at three different strain rates (approximately 10^{-3}, 10 and 3.5×10^{3} s^{-1}) using specimens with various aspect ratios (l/d=0.4, 1.0 and 1.4). The experiments were conducted in both lubricated and unlubricated conditions, and a specimen surface profile is provided. The focus of this research was comparison of plastic material behaviour across strain rates, for it is well established that high strain rate experiments do not produce an accurate representation of elastic modulus due to the time taken for wave propagation and mechanical equilibrium in the specimen. Therefore, a comparison of elastic properties at different loading rates is not discussed. If elastic properties are desired from quasi-static experiments, this would typically be achieved by using a specimen with a large l/d ratio, and measuring strain directly on the specimen surface using either a clip gauge or a suitable optical technique, such as an extensometer or speckle correlation. However, such specimens are not suitable for high strain rate experiments, nor, it will be shown later, for evaluating post-yield behaviour at low rates.

Experimental Investigations

Material Preparation and Surface Profiling

The commercial aluminium alloy AA2024 (wt%, 93.5 Al, 4.4 Cu, 1.5 Mg and 0.6 Mn), after production in wrought form, is usually subjected to heat treatment to allow for solid solution and precipitation strengthening. The resultant high strength and excellent fatigue resistance make it an ideal material in transportation applications, such as aircraft structural components.

In the present work, cylindrical specimens with a diameter of 3.5 mm were cut from an AA2024 alloy plate. Three types of compression specimens, 1.5, 3.5 and 5.0 mm in length, were prepared to produce different aspect ratios: l/d=0.4, 1.0 and 1.4, respectively. All the specimens were machined from the same region of the plate so as to minimise the effect of any microstructural differences on the mechanical response of the specimens.

Prior to mechanical testing, the surface roughness was measured to support the later experiments by providing information for interpretation of results and also characterisation for future modelling activities. The surface of a typical specimen, cleaned with isopropanol, was subjected to an ultrasonic cleaning and subsequent hot air drying. The NanoFocus μsurf™ confocal white light microscope was then employed to capture the surface topography and quantify the surface roughness.

Mechanical Testing

To achieve a wide range of strain rates, compression tests were conducted using: (1) a commercial screw driven loading machine at quasi-static (low) strain rates (~10^{-3} s^{-1}), (2) hydraulic loading machine at medium strain rates (~10 s^{-1}), and (3) split-Hopkinson pressure bars at high strain rates (~3.5×10^{3} s^{-1}) [14]. The strain rate for each test was maintained approximately constant by the prescribed velocity boundary conditions. The three groups of specimens (l/d=0.4, 1.0 and 1.4) were tested at each loading rate test to assess the specimen geometry effect on measurement accuracy and specimen response. Both lubricated (with Castrol™ LMX grease as suggested by Hall et al. [1]) and unlubricated specimens were tested for comparison purposes. At least three specimens were tested for each experiment configuration, allowing for evaluation of the test reproducibility.

In the low loading rate tests, a non-contact scanning laser extensometer (Fiedler Optoelektronik GmbH, Germany) and calibrated load cell were used to record the applied displacement and resultant force, respectively. The specimen deformation was captured using a low speed 4 megapixel camera (0.25 fps—frames per second). In the case of medium loading rates, the resisting force was obtained by means of a calibrated load cell whilst the specimen extension was measured from images produced using a Phantom™ high-speed imaging system (~50,000 fps). In the high strain rate experiments, strain gauges mounted on split-Hopkinson bars measured the stress waves in these bars, which were then used to calculate the resisting force and specimen deformation rate on the assumption of uniaxial elastic stress wave propagation as described by Harding et al. [15]. Ultra high speed photography was used to examine the deformation of a specimen using a Cordin 550 (Cordin Company, Salt Lake City, UT, USA) rotating mirror camera at a framing rate of ~250,000 fps.

From the measured force and displacement, the engineering stress and strain were calculated. Negligible difference in the stress-strain response of AA2024 was

found between tests at quasi-static and medium loading rates. Therefore only the compressive properties obtained in low and high loading rates are discussed in the following sections.

Results and Discussion

Surface Roughness

The global and local roughness profiles are illustrated in Fig. 1. Although the surface is jagged in a local vicinity of <0.5 mm [Fig. 1(b)], the specimen end is concave-shaped across 86% of the entire diameter [Fig. 1(a)]. This concavity is beneficial to hold the lubricant effectively in a compression test, thus potentially reducing the frictional effect on stress distribution [9].

The value of surface roughness depends on the scale of measurement (evaluation range). The total height (R_t) was quantified for the global and local roughness, 2.7 versus 1.7 μm, respectively, the centre-line average roughness (R_a) 0.5 versus 0.2 μm. The maximum total height of roughness (R_t=2.7 μm) over the entire end surface will lead to an error of up to 0.004 strain in compressive deformation measurement for a 1.5-mm long specimen. This error will thus reduce the accuracy of measured strains particularly in the stage of elastic deformation (elastic strain: <0.02 in AA2024).

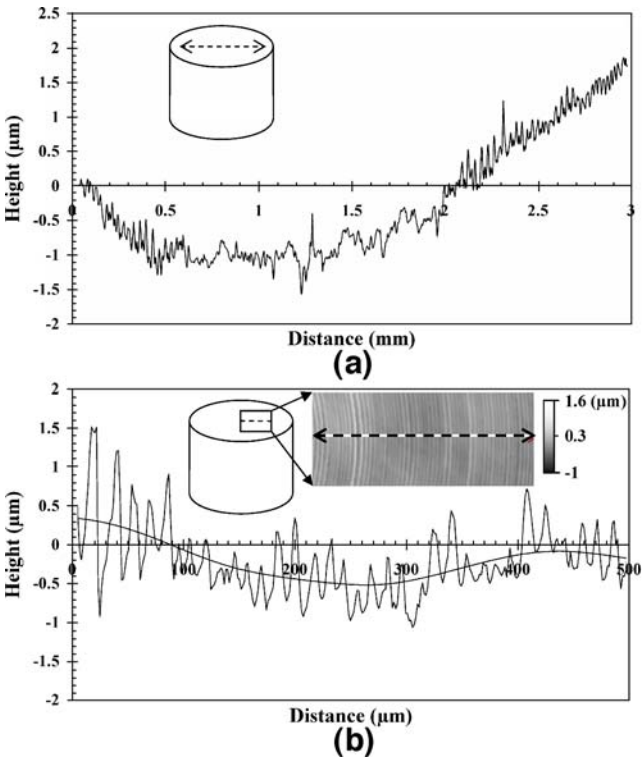

Fig. 1 The surface of a typical specimen: (**a**) global roughness and (**b**) local roughness and waveness (the dashed lines indicate where the profiles are detected)

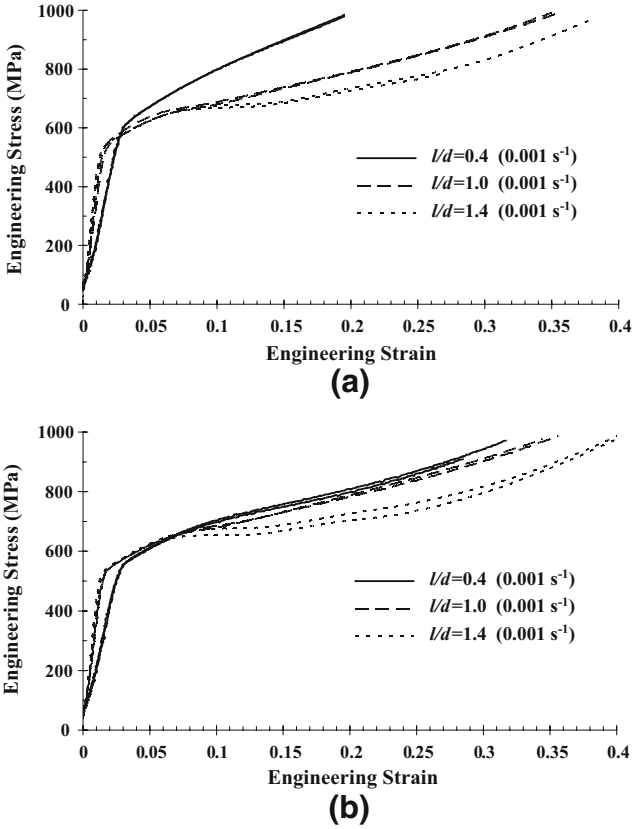

Fig. 2 Stress versus strain curve at quasi-static loading rates for the specimens: (**a**) unlubricated and (**b**) lubricated (two test repeats are marked with identical line style)

Compressive Behaviour at Low Loading Rates

The engineering stress-strain curves for AA2024 alloys at quasi-static rates of strain (~10^{-3} s^{-1}) are shown in Fig. 2. The compressive properties were measured as a function of specimen aspect ratio in lubricated and unlubricated conditions. For each test condition, a good reproducibility of better than 2% in flow stress was achieved indicative of consistent microstructure between tested specimens.

For each of the three specimen geometries, the presence or absence of lubrication has a negligible effect on the elastic region of the stress–strain curve. This can be confirmed by comparing Fig. 2(a) and (b) for each geometry. For the longer specimens (l/d=1.0 and 1.4), the flow stress and hardening behaviour are also unaffected by the presence or absence of lubricant. However, the plastic properties of the short specimen (l/d=0.4) are sensitive to lubrication. Compared to lubricated specimens, the measured resisting force dramatically increases when the specimens were unlubricated, e.g. by 8% at 0.05 strain and 20% at 0.2 strain (refer to Fig. 2 and Table 1). As

Table 1 Measured compressive properties of AA2024 alloys at quasi-static (~0.001 s^{-1}) and high (~3,500 s^{-1}) loading rates

l/d	Flow stress at ε=0.05 (±10 MPa)				Strain at failure (±0.03)
	Quasi-static		High strain rate		High strain rate
	Unlubricated	Lubricated	Unlubricated	Lubricated	Lubricated
0.4	670	620	765	670	0.78
1.0	630	625	695	670	0.46
1.4	625	625	680	665	0.27

expected, it was found that use of lubricant brings the flow stress curve of *l/d*=0.4 specimens close to that of *l/d*=1.0 samples, e.g. with the difference changed from 6% (unlubricated) to 0.8% (lubricated) at 0.05 strain; 21% to 2% at 0.2 strain (see Fig. 2 and Table 1).

In the experiments on lubricated specimens [Fig. 2(b)], the specimen geometry also affected the measurement of compressive properties. The apparent strain in short samples (*l/d*=0.4) is larger than that in other tests (*l/d*=1.0 and 1.4) for a given level of stress in the elastic region. The difference in elastic strain ($\Delta\varepsilon_e \approx 0.01$) probably results from: (1) the error in specimen length due to surface roughness and non-parallel ends; and (2) thickness of the applied lubricant layer. As discussed in the introduction, a large *l/d* ratio would be used to measure the elastic properties. Considering the larger specimens, the two aspect ratios gave indistinguishable results up to strains of ~0.08, indicating that end effects are not adversely affecting the results.

Figure 3 illustrates the recorded deformation series in lubricated quasi-static compression, in which specimens were not fractured. Almost homogeneous deformation with very little barrelling was observed in *l/d*=1.0 specimens [Fig. 3(a)]. However, localised shear slip is observed in the lubricated *l/d*=1.4 specimen. The shearing, visible in Fig. 3 between frames ε=0.05 and 0.1, arises at a strain of 0.085, and is associated with the stress drop in the stress-strain curve for all the *l/d*=1.4 specimens [Fig. 2(b)]. Because the slip occurred at the same strain in all specimens, whether lubricated or not, the authors are confident that it was not due to misalignment of the loading apparatus; rather, it is probably due to an instability caused by the intersection of the strain localisation with the sides of the specimen. The shearing slip invalidates the resisting force measurement after the strain of 0.085. Therefore the material's intrinsic mechanical properties cannot be well represented by *l/d*=1.4 specimens beyond this strain.

In summary, specimens of aspect ratio *l/d*=1.0, lubricated, give the most valid results in low loading rate compression tests. The *l/d*=0.4 specimen should be avoided due to the significant frictional effect and errors in strain measurement. The shearing slip phenomena in early stage of plastic deformation invalidates the use of *l/d*=1.4.

Compressive Behaviour at High Loading Rates

Figure 4 illustrates the engineering stress-strain curves of AA2024 at high loading rates (~3.5×10^3 s^{-1}) as a function of specimen geometry and lubrication. Similar to quasi-static strain rate tests, split-Hopkinson bar tests can be repeated with a deviation of <2%. Qualitatively, instantaneous catastrophic fracture along a shear band in the plane 45° to the loading direction occurred in all specimens at all aspect ratios; and no shearing slip was observed prior to fracture in the *l/d*=1.4 specimens, different from observations in quasi-static tests (compare Figs. 3(b) and 5).

The effects of lubrication on the high strain rate compressive properties are similar to those observed in low rate tests (compare Figs. 2 and 4). The plastic behaviour (yield strength, flow stress and hardening) of

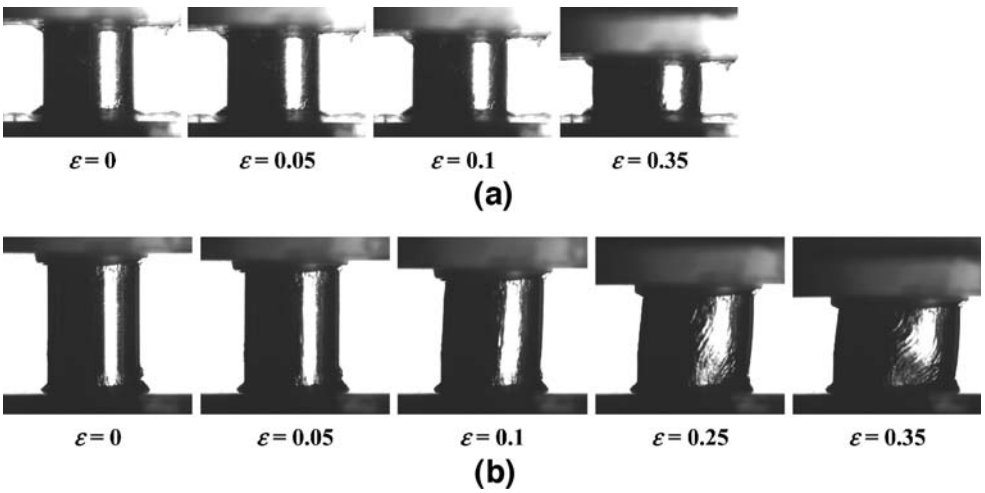

Fig. 3 Deformation sequences at quasi-static loading rates for the lubricated specimens with aspect ratio *l/d*: (**a**) 1.0 and (**b**) 1.4

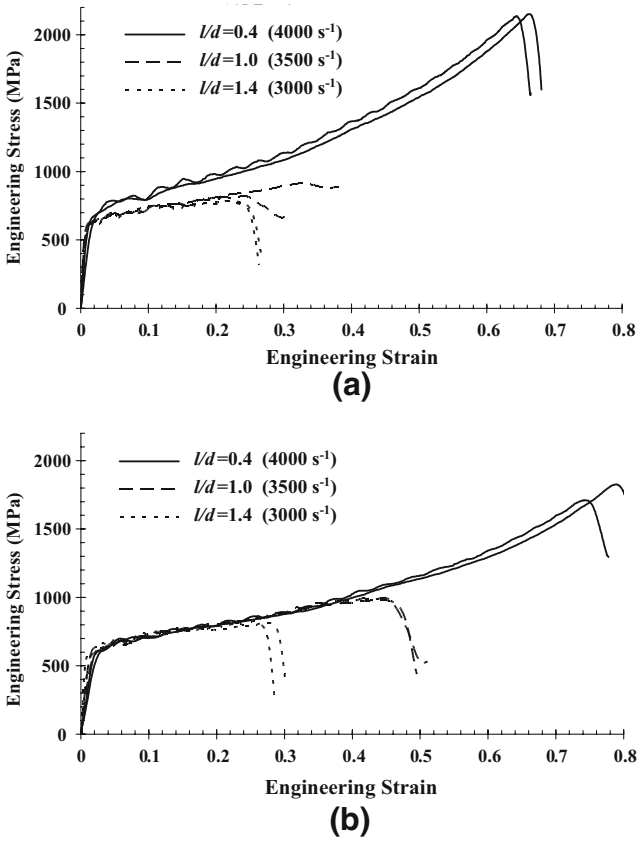

Fig. 4 Stress versus strain curve at high loading rates for the specimens: (**a**) unlubricated and (**b**) lubricated (two test repeats are marked with identical line style)

the short specimen (l/d=0.4) is sensitive to lubrication, but not in longer specimens (l/d=1.0 and 1.4). However, compared to lubricated conditions, the strain of fracture is reduced in the unlubricated tests for all aspect ratios. This is probably because the increased stress triaxiality due to friction leads to more rapid formation of shear bands in the unlubricated specimens. In a longitudinal section, the triaxial stress is a mixture of compressive and tensile nature along the diagonal (45°) whereas hydrostatic compression occurs in the centre of a specimen.

Examining the stress–strain curves for the lubricated specimens, in contrast to quasi-static loading conditions, the high rate compressive properties (i.e. yielding, hardening and flow stress) prior to fracture are not influenced by the specimen geometry (see Fig. 4 and Table 1). However, the strain at fracture increases with decreasing aspect ratio (Fig. 4 and Table 1). These data suggest that all three aspect ratios (0.4, 1.0 and 1.4) may be used to measure yield and post-yield behaviour, up to fracture, with equal confidence. Therefore, specimen choice may be based on other factors. In addition to allowing higher strain rates for a given projectile velocity in the input bar, the shorter specimens of aspect ratio l/d=0.4 are close to the ratio of 0.5 recommended for minimisation of the effects of inertia [16–19]. All three aspect ratios are less than the suggested value ($1.5<l/d<2.0$) to minimise friction in ASTM E9; however, the experiments demonstrate that friction is not a significant source of error in these conditions.

A further advantage of using smaller aspect ratios in high strain rate experiments is their ability to characterise material response to higher strains before failure occurs; the strong agreement of the results for different aspect ratios before failure indicates that the data produced are representative of intrinsic material properties, until a strain very close to the fracture strain. Such data may be required for calibration or validation of models to be used in situations where other constraints prevent material behaviour at low strains. However, it is also clear that in order to characterise fracture behaviour, it is necessary to test a number of specimens with different ratios in order to develop a range of fracture strains.

Table 2 Comparison of the effects on the measured AA2024 flow stress due to strain rates, aspect ratio and lubrication

Variable	Deviation at ε=0.05 (%)	Deviation at ε=0.2 (%)
Strain rate sensitivity	<8	<3
Test reproducibility	<2	<2
Specimen aspect ratio (unlubricated)	12	>10
Specimen aspect ratio (lubricated)	1	1
Lubrication	2–14	3–20

Sensitivity to Strain Rate, Aspect Ratio and Lubrication

To compare the intrinsic strain rate sensitivity of AA2024 alloys to factors influencing experimental accuracy (e.g. aspect ratio and lubrication), quantification was performed

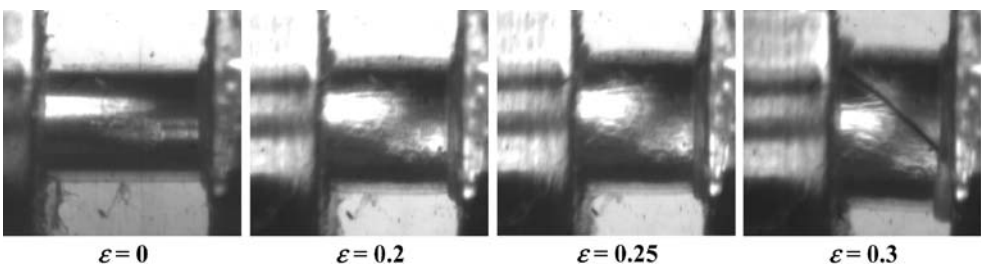

Fig. 5 Deformation sequences at high loading rates for the lubricated specimens (l/d=1.4)

to calculate the deviation from the baseline data due to experimental repeats, specimen geometry and lubrication (Table 2). The reference (baseline) stress–strain data at quasi-static and high strain rates was selected from that measured using l/d=1.0 and 0.4 lubricated specimens, respectively, on account of their capacity to characterise the intrinsic behaviour as discussed above.

The deviation value resulting from test repeatability, specimen aspect ratio and lubrication is in the same order of magnitude as strain rate sensitivity (Table 2). Specimen geometry and lubrication have a stronger impact at higher plastic strain state due to the increased stress triaxiality. This demonstrates the importance of designing a suitable specimen geometry and using the appropriate lubricant for compression tests at different loading boundary conditions.

Conclusions

The compressive behaviour of AA2024 alloys was measured as a function of three different strain rates (approximately 10^{-3}, 10 and 3.5×10^{3} s^{-1}) using lubricated/unlubricated specimens with various aspect ratios (l/d), where d=3.5 mm. The alloy shows a relatively low sensitivity to strain rate at ambient temperature, e.g. 3–8% increase in flow stress from quasi-static (~10^{-3}) to high (~3.5×10^{3} s^{-1}) strain rates.

In both quasi-static and high loading rate tests, lubrication influencing the interfacial friction has a more significant impact on the measured plastic behaviour in a short specimen (l/d=0.4) than that in long ones (l/d=1.0 and 1.4). The yield strength, hardening behaviour and flow stress value are sensitive to the specimen geometry at low loading rates, but not in high strain rate conditions. However, both the fracture strain and achievable strain rate increase with decreasing aspect ratio in the high rate tests. Quantitative analysis revealed that the effect of specimen geometry and lubrication is in the same order of magnitude as strain rate sensitivity of AA2024 alloys.

From the results presented, the following recommendations may be made regarding specimen design for yield and post-yield, pre-fracture material characterisation at different rates. An aspect ratio of 1.0 is the most suitable for quasi-static experiments. Here, larger aspect ratios may be unstable due to slip shear and shorter specimens are prone to end effects that prevent strain measurements being performed to the level of accuracy that is potentially achievable.

For high rate experiments, aspect ratios of 0.4, 1.0 and 1.4 gave essentially identical measurements of pre-fracture behaviour, and are therefore equally valid for measurements of yield and post-yield plastic deformation. Strain measurements are affected by other factors, e.g. wave propagation effects, such that the end effects, observed in quasi-static experiments, are insignificant. Therefore, in this case, considerations such as specimen inertia, achievable strain rate and desired final strain should be taken into account. These considerations would suggest that an aspect ratio of ~1.0 should be used for moderately high strain rates, and the inertia reducing aspect ratio of ~0.5 for very high rates, with some overlap between these specimen dimensions at an intermediate strain rate.

In order to characterise the rate dependence of fracture behaviour, the results indicate that it would be most suitable to perform experiments with a number of specimen aspect ratios at each of the strain rates of interest.

Acknowledgement The authors acknowledge the colleagues at University of Oxford for their help during the experiments. The Cordin 550 high speed camera used in this research was provided by the EPSRC instrument loan pool. The authors are particularly grateful to A. Walker for his advice and support whilst using this camera.

References

1. Hall IW, Guden M (2003) Split Hopkinson pressure bar compression testing of an aluminum alloy: effect of lubricant type. J Mater Sci Lett 22(21):1533–1535.
2. Li P, Maijer DM, Lindley TC, Lee PD (2007) Simulating the residual stress in an A356 automotive wheel and its impact on fatigue life. Metall Mater Trans B 38(4):505–515.
3. Spigarelli S, Evangelista E, McQueen HJ (2003) Study of hot workability of a heat treated AA6082 aluminum alloy. Scripta Mater 49(2):179–183.
4. Picu RC, Vincze G, Ozturk F, Gracio JJ, Barlat F, Maniatty AM (2005) Strain rate sensitivity of the commercial aluminum alloy AA5182-O. Mater Sci Eng A 390(1–2):334–343.
5. Field JE, Walley SM, Proud WG, Goldrein HT, Siviour CR (2004) Review of experimental techniques for high rate deformation and shock studies. Int J Impact Eng 30(7):725–775.
6. Nemat-Nasser S (2000) High strain rate tension and compression testing. In: Kuhn H, Medlin D (eds) ASM handbook, vol 8: mechanical testing and evaluation. ASM International, Materials Park, OH, pp 429–446.
7. Hartley RS, Cloete TJ, Nurick GN (2007) An experimental assessment of friction effects in the split Hopkinson pressure bar using the ring compression test. Int J Impact Eng 34(10):1705–1728.
8. Krokha VA (1974) An efficient experimental test-piece shape for compressive tests. Strength Mater 6(5):634–637.
9. Krokha VA (1978) Stresses induced in upsetting of specimens with cylindrical recesses in the end faces filled with grease. Strength Mater 10(12):1467–1471.
10. Lichtenberger A, Lach E, Bohmann A (1994) Analysis of friction in compression tests on split Hopkinson pressure bars. J Phys IV 4 (C8):29–34.
11. Trautmann A, Siviour CR, Walley SM, Field JE (2005) Lubrication of polycarbonate at cryogenic temperatures in the split Hopkinson pressure bar. Int J Impact Eng 31(5):523–544.
12. Walley SM, Radford DD, Chapman DJ (2006) The effect of aspect ratio on the compressive high rate deformation of three metallic alloys. J Phys IV 134:851–856.

13. Siebel E (1923) Grundlagen zur berechnung des kraft- und arbeitsbedarf beim schmieden und walzen. Stahl und Eisen 43:1295–1298.
14. Buckley CP, Harding J, Hou JP, Ruiz C, Trojanowski A (2001) Deformation of thermosetting resins at impact rates of strain. Part I: experimental study. J Mech Phys Solids 49 (7):1517–1538.
15. Harding J, Welsh LM (1983) A tensile testing technique for fiber-reinforced composites at impact rates of strain. J Mater Sci 18 (6):1810–1826.
16. Bertholf LD, Karnes CH (1975) 2-Dimensional analysis of split Hopkinson pressure bar system. J Mech Phys Solids 23(1):1–19.
17. Davies EDH, Hunter SC (1963) The dynamic compression testing of solids by the method of the split Hopkinson pressure bar. J Mech Phys Solids 11(3):155–179.
18. Gorham DA (1989) Specimen inertia in high strain-rate compression. J Phys D Appl Phys 22(12):1888–1893.
19. Gray GT III (2000) Classic split-Hopkinson pressure bar testing. In: Kuhn H, Medlin D (eds) ASM handbook, vol 8: mechanical testing and evaluation. ASM International, Materials Park, OH, pp 462–476.